Searching for Signatures of Internal Gamma-ray Absorption in High-redshift Blazars

A. Dmytriiev[1], A. Acharyya[2], M.Böttcher[1]

[1] NWU, Potchefstroom, South Africa, [2] CP3-origins, SDU, Odense, Denmark

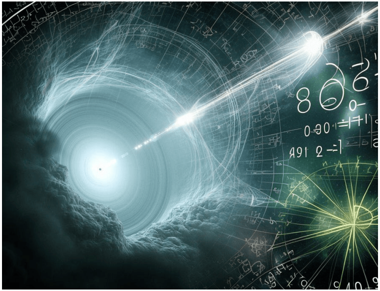

8th Heidelberg International Symposium on High-Energy Gamma-Ray Astronomy

Outline

Outline

Blazars: phenomenon and properties

Blazars – radio-loud AGN with a jet aligned with the line of sight

- non-thermal emission from radio to γ-rays
- two-bump SED
- highly variable!
  - **Flares**: flux $\nearrow$ by a factor $\sim$**10** over short time-scales minutes – weeks
  - **High states**: $t_{\rm var} \sim$ weeks – years

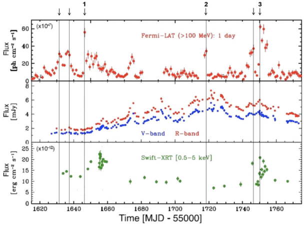

Figure: Multi-band light curves of 3C 279 variability.

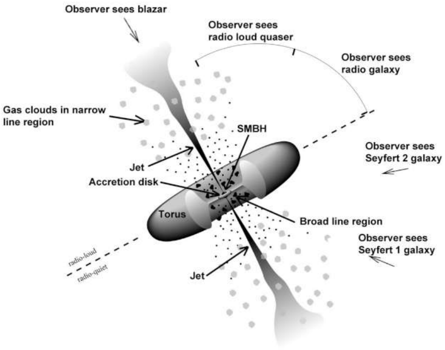

Figure: Unified view of an AGN (credit: Urry & Padovani (1995)

Spectral information: measurement of MWL SEDs

- Emitting particle spectra
- Physical conditions in the emitting zone
- MWL emission origin
- Contributions of different emission components
- Physical processes / acceleration mechanisms

Fermi-I? Fermi-II? magnetic reconnection?

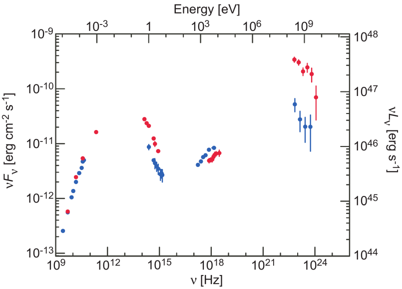

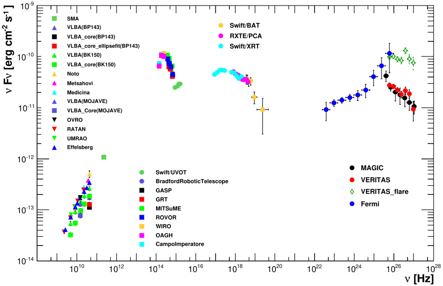

Figure: Left: nearly-simultaneous spectral measurements combined across different spectral ranges for two activity states of 3C 279 (credit: Abdo et al. (2010)). Right: multi-band spectral data of Mrk 501 taken during an observational campaign in 2009 (credit: Abdo et al. (2011)).

Different target radiation fields

Depending on location of γ-ray emitting zone in the jet, γ-rays are exposed to different photon fields:

- Accretion disk (UV, $r \lesssim 0.01$ pc)
- Broad line region (optical-UV, $r \sim 0.01 - 0.1$ pc)
- Dusty torus (infrared, $r \gtrsim 0.1$ pc)

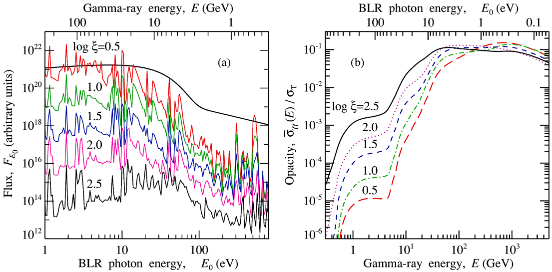

Figure: Left: typical spectrum of BLR. Right: γ-γ absorption cross-section (relative to σ_T) on BLR photon field for different energies of γ-rays. Credit: Poutanen & Stern (2010)

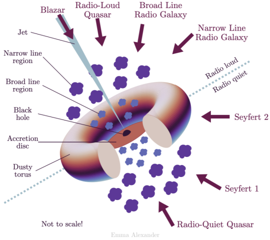

Figure: Scheme illustrating different AGN components. Credit: Emma Alexander

$\gamma - \gamma$ absorption: theory

$\gamma + \gamma \rightarrow e^- + e^+$

Threshold of pair production: $\epsilon_1\epsilon_2 \geq 2(1-\mu)^{-1}$, $\mu = \cos\theta$

Cross-section (angle-dependent):

$$\sigma_{\gamma\gamma}(\epsilon_1, \epsilon_2, \mu) = \frac{3}{16}\sigma_\mathrm{T}(1-y^2)\left([3-y^4]\times\ln\left[\frac{1+y}{1-y}\right] - 2y[2-y^2]\right)$$

with $y = \sqrt{1 - 2/(\epsilon_1\epsilon_2[1-\mu])}$

Peak in cross-section at $x = \epsilon_1\epsilon_2(1-\mu) = 4$ ($\epsilon = 2\epsilon_\mathrm{thr}$), with $\sigma_{\gamma\gamma}^\mathrm{peak} \approx 0.25\sigma_\mathrm{T}$

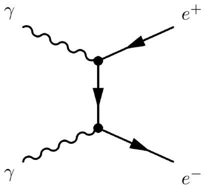

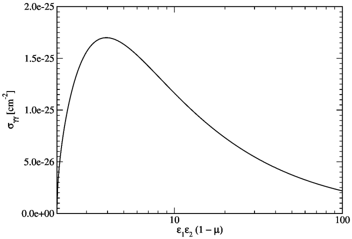

Absorption features due to different target radiation fields

Target photon fields with different spectra induce different absorption features in observed γ-ray spectra

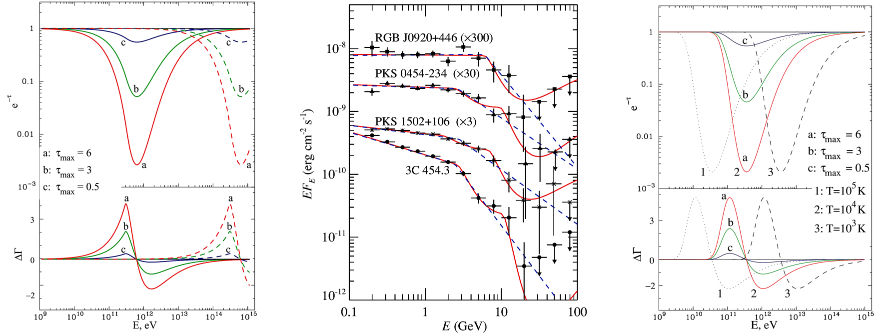

Figure: Opacity features induced by power-law seed photon field (left), BLR field (center) and blackbody (right). Credit: Poutanen & Stern (2010) and Aharonian et al. (2008)

Outline

Motivation of our study

- For high-z sources, the opacity features move to **lower energies** in the γ-ray spectra

- Interaction with **Ly α** photons (10.2 eV):
  $\boldsymbol{E_\gamma \approx 25\ \mathrm{GeV}/(1+z)}$

- For $z = (3 - 4)$:
  absorption starts from **5 – 6 GeV !**

  $\rightarrow$ best *Fermi*-LAT sensitivity !

- **Strong** optical/γ-ray signal $\rightarrow$ **high accretion disk luminosity**
  $\rightarrow$ **stronger opacity**

- **What can we learn?**
  (1) The location of γ-ray production site in the jet
  (2) Distribution of target photon fields within the source
  (3) Emission scenarios
  (4) Constraints on the opacity: how γ-rays avoid absorption?

Source selection

We select **9** γ-ray detected FSRQs with $z > 3$ (Paliya et al. (2020))

Name	R.A. (deg)	Decl. (deg)	Redshift	R_{mag}	F_{radio} (mJy)
		γ-Ray-detected blazars			
NVSS J033755−120404	54.48104	−12.06793	3.442	20.19	475.3
NVSS J053954−283956	84.97617	−28.66554	3.104	18.97	862.2
NVSS J073357+045614	113.48941	4.93736	3.01	18.76	218.8
NVSS J080518+614423	121.32575	61.73992	3.033	19.81	828.2
NVSS J083318−045458	128.32704	−4.9165	3.5	18.68	356.5
NVSS J135406−020603	208.52873	−2.10089	3.716	19.64	733.4
NVSS J142921+540611	217.34116	54.10309	3.03	19.84	1028.3
NVSS J151002+570243	227.51216	57.04538	4.313	19.89	202.0
NVSS J163547+362930	248.94681	36.49164	3.615	20.55	151.8

Fermi-LAT data analysis

Analysis: A. Acharyya

- Energy range: 0.1 GeV – 1 TeV
- **1.5 bins per decade of energy** (6 bins / 4 decades)
- 15 years of data

- Standard selection cuts
- Spectral model: 4FGL catalog shape (**power law / logparabola**)

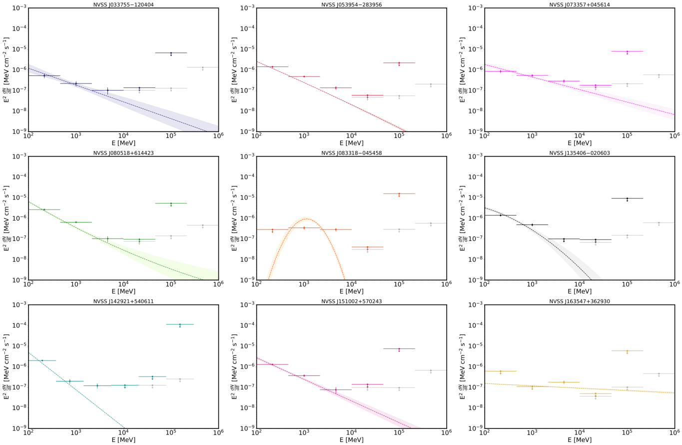

Fermi-LAT data analysis

– **2 bins per decade of energy** (used for the modeling)

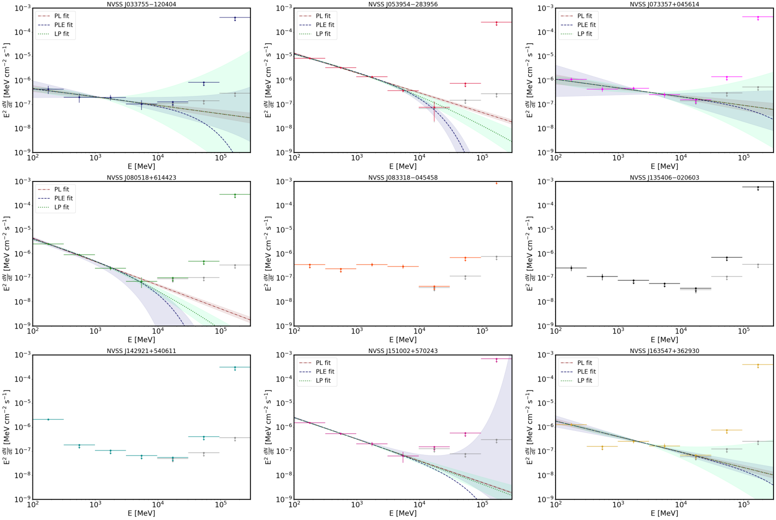

Model for γ-γ absorption in the BLR

We use the model and code by Böttcher & Els (2016)

- Full **angle-dependent** γ-γ absorption cross-section
- **BLR geometry**: a shell with inner and outer radius R_1 and R_2. Assume $u_{\rm BLR} = const$ everywhere
- Computes **optical depth τ** as a function of γ-ray energy E_γ and distance of the emitting zone from the central engine $R_{\rm ez}$

$$u_{\rm BLR} = \int_0^\infty d\epsilon \int_0^\infty dr\ 2\pi \int_{-1}^1 r^2 d\mu\ \frac{j_\epsilon(\boldsymbol{r})}{4\pi r^2 c} = \frac{1}{2c}\int_0^\infty d\epsilon\ j^0_\epsilon \int_{-1}^1 d\mu\ D(\mu)$$

$$\tau_{\gamma-\gamma}(\epsilon_\gamma, d) = \frac{1}{2c}\int_{R_{\rm ez}}^\infty dl \int_{-1}^1 d\mu \int_0^\infty d\epsilon\ \frac{j^0_\epsilon D(\mu)}{\epsilon m_{\rm e} c^2} \times (1-\mu_i)\ \sigma_{\gamma-\gamma}(\epsilon_\gamma, \epsilon, \mu_i)$$

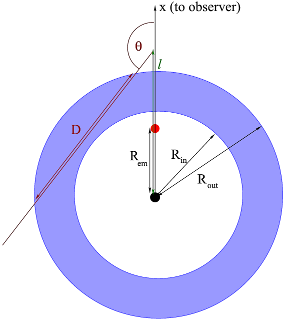

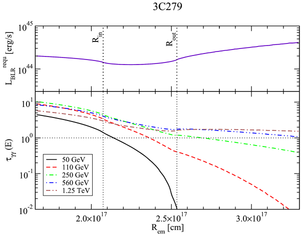

Target radiation field: $u_{\nu,\mathrm{rad}}(\nu)$

We use a template for BLR spectrum with a **blackbody continuum** ($T = 1500$ K) and a **set of 4 emission lines** as measured in real optical data. We assume that the total BLR luminosity (sum of 4 lines + continuum) is (always) 10% of L_D

$$u_\mathrm{line} = \frac{L_\mathrm{line}}{4\pi R_\mathrm{BLR}^2 c} \qquad u_\mathrm{cont} = u_\mathrm{BLR,tot} - \frac{\Sigma L_\mathrm{line}}{4\pi R_\mathrm{BLR}^2 c} \qquad u_\mathrm{BLR,tot} = \frac{0.1 L_\mathrm{D}}{4\pi R_\mathrm{BLR}^2 c}$$

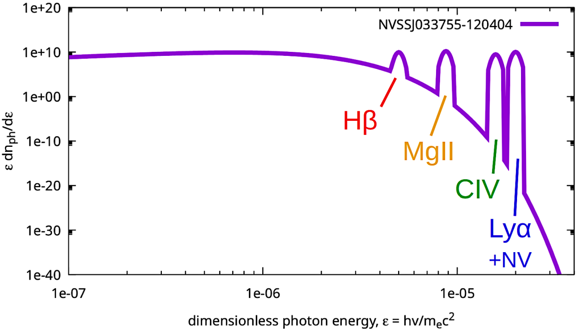

Luminosity of the accretion disk

We assume that the **BLR** dominates the target radiation field, with the BLR covering fraction 10%

$$u_{\mathrm{BLR,tot}} = \frac{0.1 L_{\mathrm{D}}}{4\pi R_{\mathrm{BLR}}^2 c}$$

$$R_{\mathrm{BLR}} \approx 0.1\ L_{\mathrm{D},46}^{1/2}\ \mathrm{pc}$$

e.g. Hayashida et al. (2012)

We adopt L_{D} from Paliya et al. (2020) – estimates based on broadband SED modeling

Source #	Name (NVSS)	log10(L_{D} erg s^{-1})
1	NVSS J033755-120404	46.36
2	NVSS J053954-283956	46.70
3	NVSS J073357+045614	46.60
4	NVSS J080518+614423	46.34
5	NVSS J083318-045458	47.15
6	NVSS J135406-020603	46.78
7	NVSS J142921+540611	46.26
8	NVSS J151002+570243	46.63
9	NVSS J163547+362930	46.30

Luminosity of optical BLR emission lines

- We use available luminosities of the most prominent optical emission lines
- **Lyα** (1216 Å) **+ N V** (1240 Å), **C IV** (1549 Å), **Mg II** (2798 Å) and **Hβ** (4861 Å)
- Need to know $L_{\mathrm{Ly}\alpha}$ (+N V) very accurately
  $\rightarrow$ induces opacity features at lowest γ-ray energies
- We adopt L_{MgII} and $L_{\mathrm{H}\beta}$ from an IR study by Burke et al. (2024)
- We adopt L_{CIV} from Paliya et al. (2021) (except source #3)
- **For $L_{\mathrm{Ly}\alpha}$** (includes N V):
  - source #1, 2: old measurements from Osmer et al. (1994) only
  - source #3: prediction derived using scaling as by average ratios of Francis et al. (1991) (as well as for L_{CIV})
  - source #4, 5: no information at all (and the measured line ratios are *inconsistent* with Francis et al.)
  - source #6, 7, 8, 9: accurate measurement through **SDSS DR18**

Luminosity of optical BLR emission lines

Source #	Name (NVSS)	z	log10($L_{\mathrm{Ly}\alpha+\mathrm{NV}}$)	log10(L_{CIV})	log10(L_{MgII})	log10($L_{\mathrm{H}\beta}$)
1	J033755-120404	3.442	44.8941	44.268 ± 0.193	44.73 ± 0.09	44.24 ± 0.05
2	J053954-283956	3.104	44.7335	45.091 ± 0.091	44.38 ± 0.04	43.21 ± 0.09
3	J073357+045614	3.01	44.613 ± 0.063	44.412 ± 0.063	44.09 ± 0.02	44.01 ± 0.06
4	J080518+614423	3.033	x	44.743 ± 0.095	44.39 ± 0.03	43.79 ± 0.06
5	J083318-045458	3.5	x	45.220 ± 0.111	44.63 ± 0.01	44.47 ± 0.01
6	J135406-020603	3.716	45.092 ± 0.027	44.552 ± 0.038	44.39 ± 0.06	43.95 ± 0.09
7	J142921+540611	3.03	44.36 ± 0.04	44.241 ± 0.018	44.07 ± 0.09	43.79 ± 0.11
8	J151002+570243	4.313	45.245 ± 0.019	44.857 ± 0.059	44.84 ± 0.09	x
9	J163547+362930	3.615	44.8 ± 0.22	44.305 ± 0.023	44.42 ± 0.02	43.75 ± 0.04

Approach

- We **fit** each spectrum with a **power law** or **logparabola** (4FGL catalog shape)
- We γ-γ **absorb** each model using the opacity code (with the relevant $L_{\rm D}$), while varying the location of the γ-ray production region
- Folded model (average over bins): $\chi^2 \leq \chi^2_{\rm min} + 1$ indicates allowed locations in the jet (1σ)

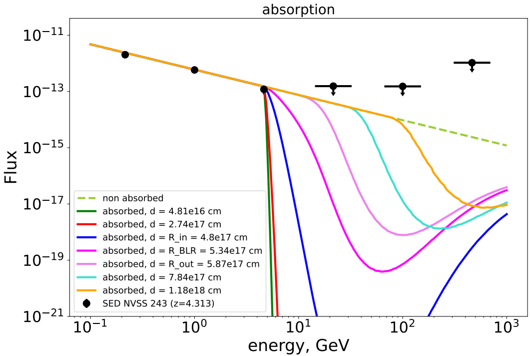

Fit results

- 3/9 sources do not have enough statistics
- Of remaining 6 sources, 5 have Lyα information available
- **Lower limit** of distance from SMBH (only) for 4/9 sources
- Spectrum of Source #3 is **consistent with opacity model**

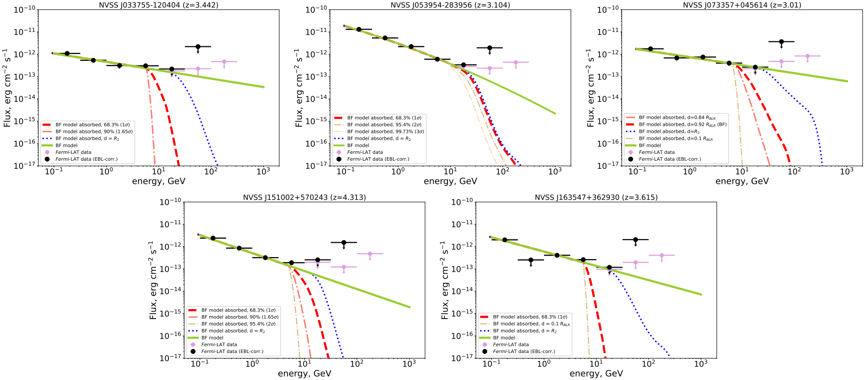

Constraints on the γ-ray production zone location

Source #	Name (NVSS)	$R_{\rm BLR}$ (cm)	$R_{\rm ez}/R_{\rm BLR}$ (1σ)	... (1.65σ)	χ^2_ν (non-abs)
1	J033755-120404	4.67×10^{17}	$\geq$ **0.92**	≥ 0.48	2.43/2
2	J053954-283956	6.9×10^{17}	$\geq$ **1.08**	≥ 1.06	3.84/2
3	J073357+045614	6.16×10^{17}	= **0.92**	=	5.13/2
4	J080518+614423	–	–	–	–
5	J083318-045458	–	–	–	–
6	J135406-020603	–	–	–	–
7	J142921+540611	–	–	–	–
8	J151002+570243	6.37×10^{17}	$\geq$ **1.01**	≥ 0.92	2.57/2
9	J163547+362930	4.36×10^{17}	$\geq$ **0.84**	NA	0.76/1

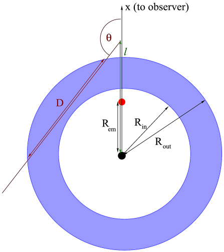

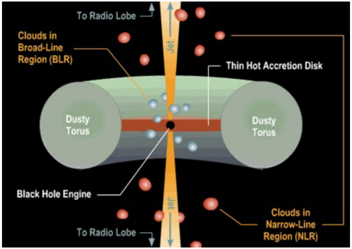

Particular case: Source #3

- Spectrum of Source #3 is **consistent with opacity model**
- An improved χ^2 ($\Delta\chi^2 < 0$) is achieved for the **absorbed model** in the range $\boldsymbol{R_{\rm ez}/R_{\rm BLR} \geq 0.84}$
- The best fit is achieved for $\boldsymbol{R_{\rm ez}/R_{\rm BLR} = 0.92}$ $\rightarrow$ emitting zone WITHIN BLR

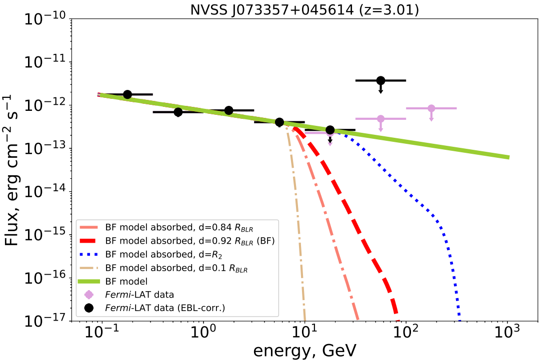

Discussion of results

- **The observed cutoff in the γ-ray spectra cannot be distinguished from e.g. cutoff in the particle spectrum** $\rightarrow$ mostly lower limits on the emitting zone location

- Very particular location – shocked region in the jet consistently in the vicinity of BLR shell

  The emitting zone **cannot be too far** from BLR as well $\rightarrow$ production of γ-rays via IC

- **Source #2 (NVSS J053954-283956)** – tighter constraints can be derived (emitting zone close to inner BLR radius)

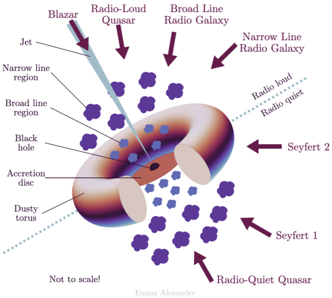

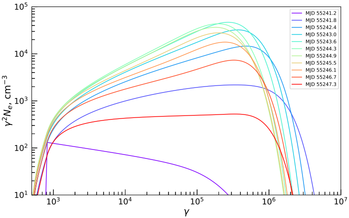

Discussion of results

- **Second emitting zone?**
  – full physical modeling required
  – correlation between different bands

- Hadronic models
  – p-γ process – internal opacity

- Exotic physics, e.g. **photon-axion coupling in magnetic field** ?

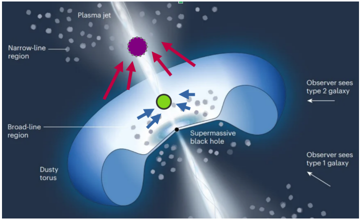

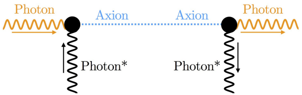

Outline

Constraining the EBL

- The best-fit χ^2 for the **EBL-deabsorbed** intrinsic spectrum for different EBL models (Saldana-Lopez 2021; Finke 2022; Franceschini 2018; ...)
  - limited statistics of the data
  - full physical modeling is preferred
- **Statistical approach**: spectral index as a function of redshift z
  - limited selection of sources

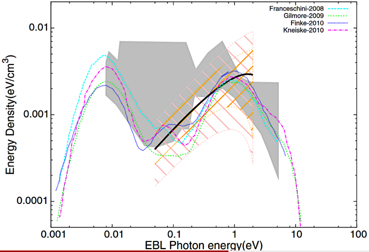

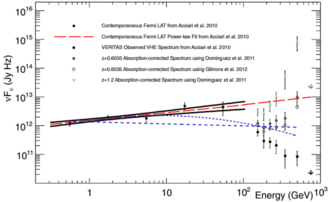

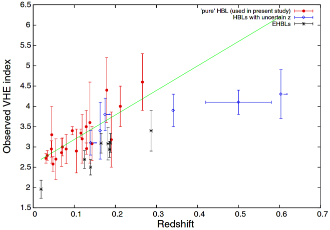

Figure: (Top): example of de-absorption of an observed γ-ray spectrum using different EBL models (Furniss et al. 2013). Bottom: distribution of observed VHE spectral index of a selection of HBLs as a function of redshift (Sinha et al. 2014)

Studying internal absorption in other blazars

- **Intermediate redshift blazars (z=1–2)**: an optimal balance between the γ-ray statistics and the opacity feature downshift

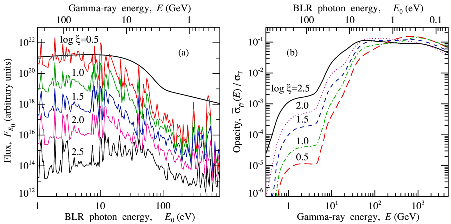

Figure: Left: typical spectrum of BLR. Right: γ-γ absorption cross-section (relative to σ_{T}) on BLR photon field for different energies of γ-rays.
Credit: Poutanen & Stern (2010)

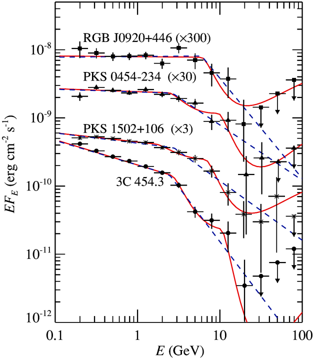

Figure: Opacity features induced by the BLR field (Poutanen & Stern (2010))

Beyond leptonic models: hadronic scenario

$$\pi^{\pm} \rightarrow \mu^{\pm} + \nu_{\mu}(\bar{\nu}_{\mu})$$
$$\mu^{\pm} \rightarrow e^{\pm} + \bar{\nu}_{\mu}(\nu_{\mu}) + \nu_{e}(\bar{\nu}_{e})$$

TXS 0506+056

– IceCube $\sim$ 290 TeV ν (2017)
 + GeV (*Fermi*-LAT) and VHE (MAGIC) flare
– ν-flare (2014 – 2015): no γ-ray activity

Assuming **photo-hadron** (rather than *p*-*p*):

$$E'_{\nu} \approx 0.05 E'_{\mathrm{p}}, \quad s \approx E'_{\gamma} E'_{\mathrm{p}} \approx E^2_{\Delta^+}$$

- **Target field: X-ray** (Böttcher et al. (2022))
- Synchrotron-supported cascade is ruled out (Reimer et al. (2019))

⇒ Target photons originate outside the jet?

! GeV γ-rays **absorbed** on the target field

→ **Strong ν sources: WEAK at GeV γ-ray !**

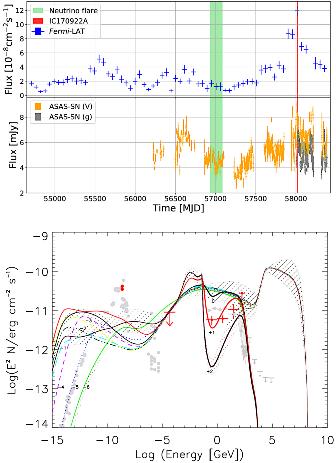

Figure: (Top) *Fermi*-LAT and optical LC of TXS 0506+056. Green – neutrino flare in 2014 – 2015. (Bottom) Simulations of synchrotron-supported cascades to generate the observed neutrino flare flux (credit: Reimer et al. (2019))

Prospects with CTA

The next generation IACT instrument. Operational by 202**?**

LST particularly helpful thanks to the low-energy threshold and sensitivity

- Sensitivity $\nearrow$ by a factor of $\sim$ **10**
- Northern and Southern site (La Palma and Chile)
- Energy range: $\sim$**30 GeV** – $\sim$**300 TeV**
- Substantially better angular, spectral and timing resolution

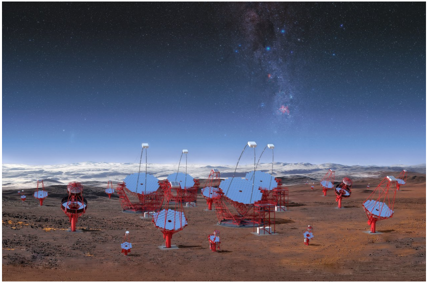

Figure: CGI rendering of the CTA array view (credit: ESO/CTA)

$\rightarrow$ **Much tighter constraints on opacity, γ-ray production region location and EBL**

Outline

Summary

- **Exploring high-redshift blazars allows to search for γ-γ opacity signatures at lower energies**

- We established **constraints on the location of the γ-ray production region** in the jet for 5 blazars with redshifts z = 3 – 4.3

- One needs to understand why the γ-ray production (shocked region in the jet) takes place mostly close to the **BLR outer boundary**

- One of the sources displays a possible **$\gamma - \gamma$ opacity feature** at energy $\sim$ **8 GeV**. **Emitting zone located within the BLR close to the INNER boundary**

- Full modeling required – leptonic, hadronic, multi-zone models

- Promising prospects with CTA

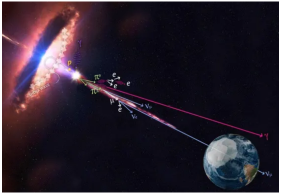

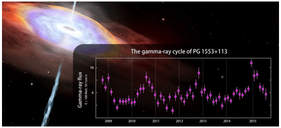

$\Rightarrow$ ApJ paper in preparation, to be submitted (hopefully) within this month

Thank you!